DOI 10.5012/bkcs.2010.31.7.1941

Visible-light Photocatalytic Activity of $BiOCl/Bi_3O_4Cl$ Nanocomposites

Bifen Gao, Ashok Kumar Chakraborty, Ji Min Yang,† and Wan In Lee*

*Department of Chemistry, Inha University, Incheon 402-751, Korea. *E-mail: wanin@inha.ac.kr*
†Indian Springs School, Indian Springs, Alabama 35124, U.S.A.
Received March 10, 2010, Accepted May 28, 2010

The heterojunction structures of $BiOCl/Bi_3O_4Cl$, exhibiting considerable visible-light photocatalytic efficiency, were prepared by a simple wet-chemical process at ambient condition. The prepared nanocomposites were characterized by XRD, TEM, and UV-visible diffuse reflectance spectra. Under visible light ($\lambda \geq 420$ nm) irradiation, $BiOCl/Bi_3O_4Cl$ exhibited an enhanced photocatalytic activity in decomposing 2-propanol (IP) in gas phase and salicylic acid (SA) in aqueous solution, whereas the bare BiOCl and Bi_3O_4Cl showed negligible activities. It is deduced that the remarkable visible-light photocatalytic activity of the $BiOCl/Bi_3O_4Cl$ originates from the hole (h^+) transfer between VB of the Bi_3O_4Cl and BiOCl semiconductors.

Key Words: Photocatalyst, Visible light, BiOCl, Bi_3O_4Cl, Heterojunction

Introduction

Removal of organic compounds with heterogeneous photocatalysts, utilizing solar light, attracts augmenting attention as an environmentally benign technology for the treatment of contaminants in air and water.[1-4] The applications of various semiconductors as photocatalyst have been extensively investigated thus far,[5-7] and undoubtedly, TiO_2 has been accepted as the most efficient photocatalyst for the degradation of organic compounds under UV irradiation.[8-10] Due to the large bandgap ($E_g = 3.2$ eV), however, TiO_2 can utilize only the photons in the UV region ($\lambda \leq 380$ nm), which limits the practical application of TiO_2 in solar light or indoor. Therefore, the development of new photocatalytic systems, which are active in a wide range of visible light, will be indispensable for the commercialization of photocatalysts.

Recently, the Sillén family compounds with unique layered structure have often been investigated as photocatalyst.[11,12] It was reported that the internal static electric field perpendicular to each layer in these structures could induced the effective separation of photo-generated electron-hole pairs, and a high photocatalytic performance as a result.[11,12] Bi_3O_4Cl is a simple member of the Sillén family with the $[Bi_3O_4]$ and [Cl] layers one by one orderly piled up along the c-axis to form a unique layered structure. Huang *et al*. has reported the photocatalytic degradation of methyl orange in water by Bi_3O_4Cl under visible light irradiation, since the bandgap of Bi_3O_4Cl is only 2.79 eV.[13] Contrarily, BiOCl with large bandgap ($E_g = 3.6$ eV) does not exhibit any photocatalytic activity under visible light, but it was reported that it reveals excellent photocatalytic activity for degradation of organic dyes under UV irradiation.[14] Recently, an efficient heterojunctioned photocatalyst, $BiOCl/Bi_2O_3$, working under visible light in decomposing organic pollutants in gas and aqueous phases has been developed.[15] In this $BiOCl/Bi_2O_3$ system, the BiOCl works as main photocatalyst, while the role of Bi_2O_3 is a sensitizer absorbing visible light. Herein, we report the heterojunctioned $BiOCl/Bi_3O_4Cl$ systems, which are expected to present visible light photocatalytic efficiency based on similar principle. The $BiOCl/Bi_3O_4Cl$ composites in various compositions were prepared by a simple chemical solution process, and were applied to decompose 2-propanol (IP) in gas phase and salicylic acid (SA) in aqueous solution under visible light irradiation.

Experimental Section

Synthesis of BiOCl. $Bi(NO_3)_3{\cdot}5H_2O$ (0.01 mol) was dissolved in 200 mL 1.0 M nitric acid aqueous solution under magnetic stirring. By the subsequent addition of 10 mL 6.0 M hydrochloric acid to this solution, a white precipitate was formed immediately. After magnetic stirring for 2 hr, the precipitate was centrifuged and washed with deionized water three times. Finally, the white powdered BiOCl was obtained by drying the precipitate at 100°C for 24 hr.

Synthesis of Bi_3O_4Cl. Bi_3O_4Cl powder with pale-yellow color was synthesized by the solid-state reaction with Bi_2O_3 and BiOCl.[13] 0.010 mol BiOCl powder obtained by the above procedure and 0.010 mol Bi_2O_3 (Aldrich) were mixed in a mortar, and subsequently annealed at 700 °C for 6 hr. The crystallographic phase and purity of the Bi_3O_4Cl samples were identified by XRD.

Synthesis of $BiOCl/Bi_3O_4Cl$ composites. The as-prepared 0.010 mol Bi_3O_4Cl powder was suspended in 100 mL ethanol, and the stoichiometric amounts of 6.0 M aqueous HCl were added at room temperature, to convert Bi_3O_4Cl partially to BiOCl. The composition of BiOCl was determined by the added molarity of HCl. Typically, for the formation of 47/53 $BiOCl/Bi_3O_4Cl$ (47% of BiOCl and 53% of Bi_3O_4Cl), 7.0 mL of HCl was added. After a virgorous stirring for 3 h, the prepared $BiOCl/Bi_3O_4Cl$ in ethanol solution was centrifuged and washed with ethanol several times. Finally, the composites were dried overnight at 100 °C.

Characterization. X-ray diffraction patterns of the $BiOCl/Bi_3O_4Cl$ composites were obtained by using a Rigaku Multiflex diffractometer with monochromated high-intensity Cu Kα radiation. UV-visible diffuse reflectance spectra were acquired by using a Perkin-Elmer Lambda 40 spectrophotometer. $BaSO_4$ was used as the reflectance standard. The sizes and morpho-

logies of the composites were observed by SEM (Hitachi, S-4300) and TEM (Philips CM30). For the TEM analysis, ethanol suspensions of the BiOCl/Bi_3O_4Cl particles were spread on a copper grid coated with holey amorphous carbon film.

Evaluation of photocatalytic activity. The as-prepared BiOCl/Bi_3O_4Cl samples were tested as photocatalyst for the decomposition of 2-propanol in gas phase. For the photocatalytic measurements, an aqueous suspension containing 5×10^{-5} mol of the BiOCl/Bi_3O_4Cl composites were spread on a 2.5×2.5 cm^2 Pyrex glass in a film form, which was subsequently dried at 50 °C for 2 hr. The gas reactor system used for this photocatalytic reaction was described elsewhere.[16] The net volume of the gas-tight reactor was 200 mL, and the BiOCl/Bi_3O_4Cl particulate film was located at the center of the reactor. A 300 W Xe lamp was employed as the light source. The light beam passed through a UV cut-off filter (≤ 420 nm, Asahi) and a water filter to remove the IR component. After evacuation of the reactor, 0.08 mL of 2-propanol mixed in 1.6 mL of water was injected into the reactor. Then the initial concentration of gaseous 2-propanol in the reactor was kept to 117 ppm in volume (ppmv). Thus the ultimate concentration of CO_2 evolved will be 351 ppmv when the whole 2-propanol is completely decomposed, as shown in the following equation.

$$2\ (CH_3)_2CHOH\ (g) + 9\ O_2\ (g) \rightarrow 6\ CO_2\ (g) + 8\ H_2O\ (g)$$

The total pressure of the reactor was then controlled to 750 Torr by the addition of oxygen gas. Under these conditions, 2-propanol and H_2O remained in the vapor phase. After a certain time of irradiation, 0.5 mL of the gas in the reactor was automatically picked up and sent to a gas chromatograph (Agilent Technologies, Model 6890N). For the detection of CO_2, a methanizer was installed between the GC column outlet and the FID detector.

For the degradation of salicylic acid (SA) in aqueous solution, 1×10^{-4} mol of the BiOCl/Bi_3O_4Cl composite sample was dispersed in 50 mL SA aqueous solution (5×10^{-5} M) by magnetic stirring. The remnant salicylic acid after the irradiation of visible light ($\lambda \geq 420$ nm) was analyzed from its characteristic absorption peak detected by UV-visible spectrophotometer (PerkinElmer Lambda 40).

Results and Discussion

The BiOCl/Bi_3O_4Cl composites were prepared by the three-step reactions described as follows. First, the BiOCl powder was formed by the reaction of $Bi(NO_3)_3 \cdot 5H_2O$ and HCl at ambient condition. Second, the crystallized Bi_3O_4Cl with pale-yellow color was synthesized by the solid-state reaction with Bi_2O_3 and BiOCl at 700°C. Finally, BiOCl/Bi_3O_4Cl composites were prepared by treating Bi_3O_4Cl with the stoichiometric amounts of aqueous HCl at room temperature, as described in Scheme 1. The pale yellow color of Bi_3O_4Cl was changed to white, suggesting that the surface of Bi_3O_4Cl was converted to BiOCl.

The crystallographic phases and compositions of the as-prepared BiOCl, Bi_3O_4Cl and several BiOCl/Bi_3O_4Cl composites were analyzed by XRD. As shown in Figure 1, the BiOCl prepared at the initial step is in the pure and highly crstallized phase.

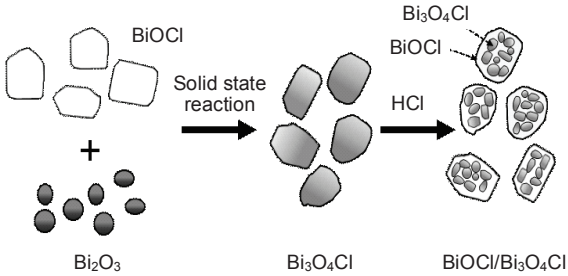

Scheme 1. Preparation route for the BiOCl/Bi_3O_4Cl composite.

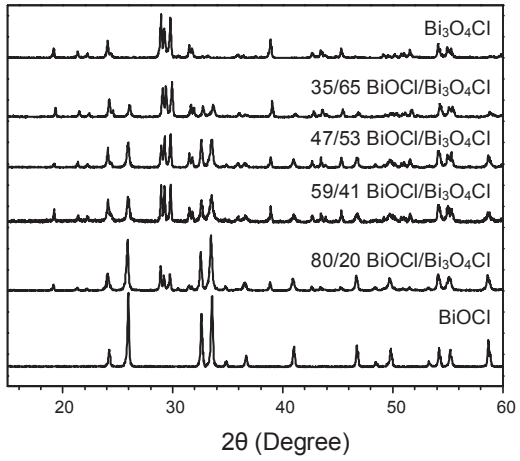

Figure 1. XRD patterns for the synthesized BiOCl, Bi_3O_4Cl, and the several BiOCl/Bi_3O_4Cl composites.

All the diffraction peaks were assigned to the tetragonal BiOCl phase (P4/nmm space group, JCPDS: 73-2060), in which the [BiOCl] layers are stacked along the c-axis with van der Waals interaction of [Cl] to form a unique layered structure.[14] For the Bi_3O_4Cl derived from the solid-state reaction of BiOCl and Bi_2O_3 at 700 °C, all the diffraction peaks corresponded to the monoclinic phase (I2/a space group, JCPDS: 86-2221).[13] In the several BiOCl/Bi_3O_4Cl composites, both the tetragonal BiOCl and monoclinic Bi_3O_4Cl phases appeared, but other impurity phases were not detected at all. With increasing the molarity of HCl in the reaction of Bi_3O_4Cl and HCl, the intensities of the characteristic BiOCl peaks were increased, whereas those of Bi_3O_4Cl were decreased. The relative compositions of BiOCl and Bi_3O_4Cl can be determined by analyzing the integrated areas of the main XRD peaks for both phases.[17] Herein, the (011) peak of BiOCl and (114) peak of Bi_3O_4Cl were used to estimate the relative composition of the BiOCl/Bi_3O_4Cl composites.

The structure of the 47/53 BiOCl/Bi_3O_4Cl was examined by TEM, as shown in Figure 2a. The shape and size of the composite did not seem to be uniform, but its size was about 1 μm in average. It is considered that BiOCl occupies the surface of 47/53 BiOCl/Bi_3O_4Cl, as shown in Scheme 1, since the surface will have higher opportunity to react with the added HCl.[15] High resolution TEM image in Figure 2b, also suggests that the Bi_3O_4Cl nano-grains are embedded in the BiOCl matrix. The lattice spacings of 0.30 nm and 0.31 nm correspond to the (114) and (006) plane of monoclinic Bi_3O_4Cl, whereas those of 0.26 nm and 0.27 nm can be indexed as the (012) and (110)

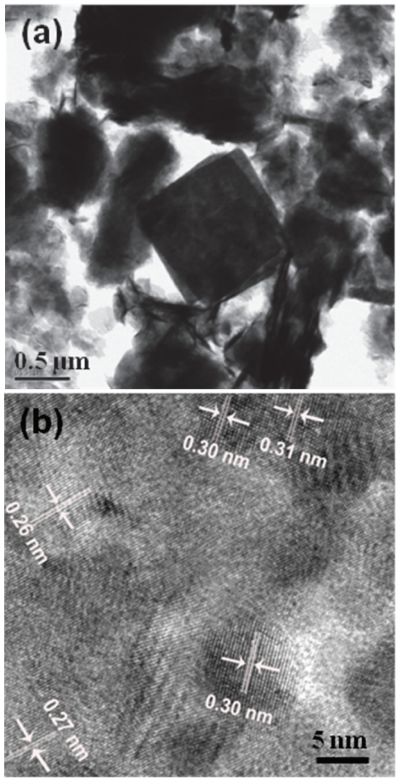

Figure 2. Low (a) and high (b) magnification TEM images for the 47/53 BiOCl/Bi_3O_4Cl composite.

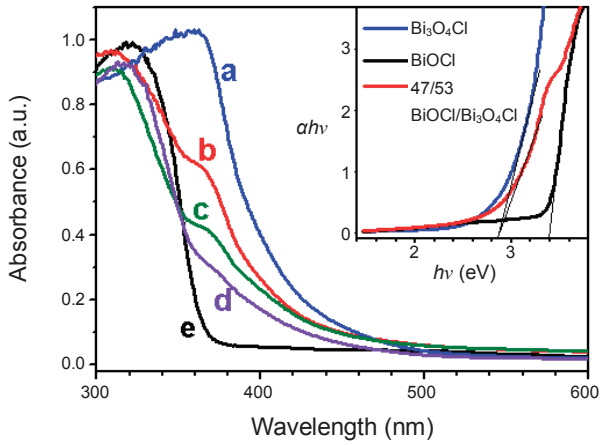

Figure 3. Diffuse reflectance spectra for BiOCl, Bi_3O_4Cl, and the several BiOCl/Bi_3O_4Cl composites. a, Bi_3O_4Cl; b, 47/53 BiOCl/Bi_3O_4Cl; c, 59/41 BiOCl/Bi_3O_4Cl; d, 80/20 BiOCl/Bi_3O_4Cl; e, BiOCl. Plots of $\alpha h\nu$ *vs*. irradiated light energy in eV were shown in the inset. *a*, *h*, *v* are absorption coefficient, Planck constant, and light frequency, respectively.

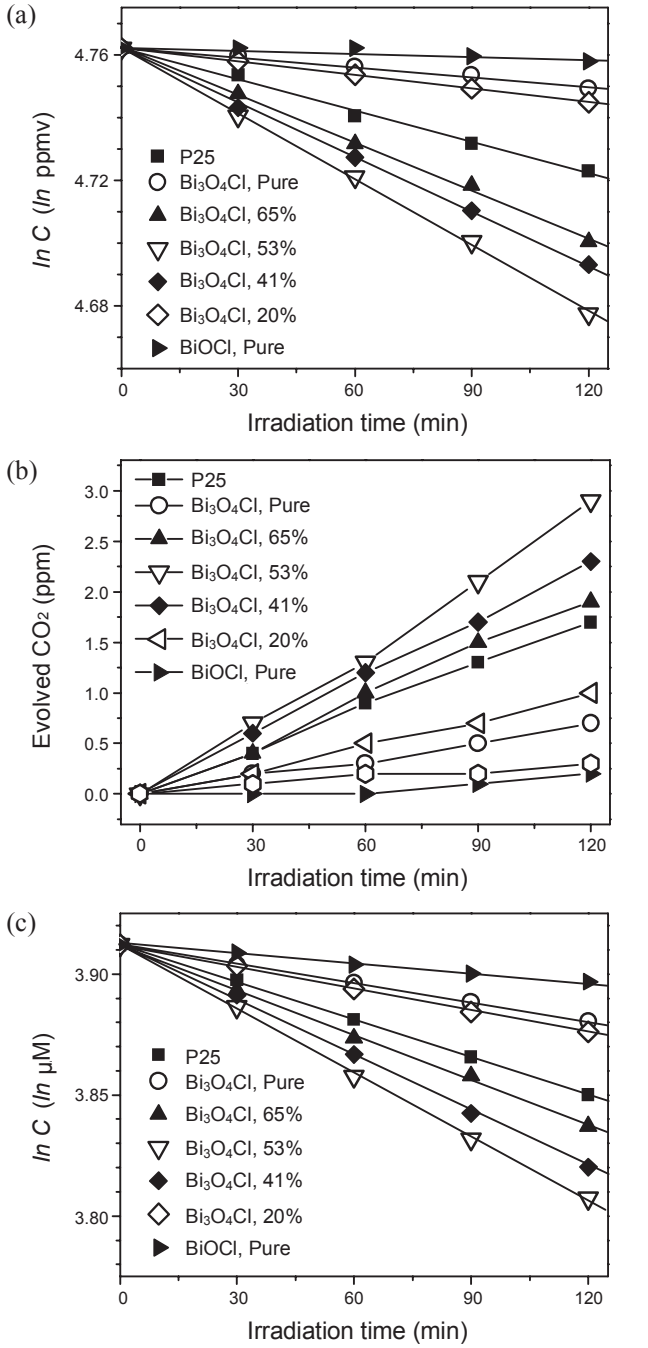

Figure 4. Photocatalytic removal of gaseous IP (a) and CO_2 evolved (b) with the BiOCl, Bi_3O_4Cl, and the several BiOCl/Bi_3O_4Cl composites under visible light irradiation ($\lambda \geq 420$ nm). (c) Photocatalytic degradation of aqueous SA *vs*. irradiation time with suspensions of the photocatalytic samples under visible light irradiation ($\lambda \geq 420$ nm).

planes of the tetragonal BiOCl crystal. This clearly indicates that a tight heterojunction has been formed between BiOCl and Bi_3O_4Cl in a nano-size level.

Figure 3 shows the diffuse reflectance spectra of the as-prepared BiOCl, Bi_3O_4Cl, and several BiOCl/Bi_3O_4Cl composites with different concentration of Bi_3O_4Cl. The band gap (E_g) of BiOCl and Bi_3O_4Cl, determined by the extrapolation to the zero absorption coefficient, were 3.4 eV and 2.85 eV, respectively, corresponding to the previous reports.[18-20] The BiOCl/Bi_3O_4Cl composites showed the dual absorption edges at 360 nm and 435 nm, indicating the presence of BiOCl and Bi_3O_4Cl. The absorbance in the 370 - 430 nm range was gradually increased, as the component of Bi_3O_4Cl phase increased in the BiOCl/Bi_3O_4Cl.

For the evaluation of the photocatalytic efficiencies for the Bi_3O_4Cl, BiOCl and several BiOCl/Bi_3O_4Cl composites, 2-propanol (IP) in gas phase was employed as a model compound. As shown in Figure 4a, the photocatalytic decomposition of IP

was plotted as *ln C vs*. irradiation time with an approximation of first order kinetics. That is, the catalytic reaction can simply be described by $-d[c]/dt = k[c]$, where [c] is the concentration of gaseous IP, t is the irradiation time and k is the overall degradation rate constant. The BiOCl/Bi_3O_4Cl composites exhibited considerable enhancement in the photocatalytic removal of IP, whereas the end-members showed the negligible efficiency. Especially, 47/53 BiOCl/Bi_3O_4Cl demonstrated the highest catalytic efficiency. After 2 hr of visible light ($\lambda \geq 420$ nm) irradiation, k of the 47/53 BiOCl/Bi_3O_4Cl composite was 6.6 times that of Bi_3O_4Cl, and 2.1 times that of Degussa P25.

The BET surface areas of BiOCl and Bi_3O_4Cl were determined to be 3.82 and 3.19 m^2/g, respectively, while that of 47/53 BiOCl/Bi_3O_4Cl was 3.45 m^2/g. The measured surface area of 47/53 BiOCl/Bi_3O_4Cl was less than 1/10 that of the Degussa P25 TiO_2 (47 m^2/g), but its photocatalytic efficiency was more than twice, suggesting that the achieved photocatalytic activity is noticeably high.

In evolution of CO_2, the similar trend was also observed, as shown in Figure 4b. It was found that the CO_2 evolved in 2 hr of the visible irradiation with 47/53 BiOCl/Bi_3O_4Cl was ~4 times that with pure Bi_3O_4Cl, and 1.7 times that with Degussa P25. It is clearly indicated that the complete mineralization of IP into inorganic substances is possible by this heterojunction structure.

The photocatalytic activity of BiOCl/Bi_3O_4Cl was also evaluated according to the removal of SA in aqueous solution. The remnant SA after the irradiation of visible light ($\geq$ 420 nm) was analyzed from its characteristic absorption peak by UV-visible spectroscopy. With approximating the photocatalytic degradation of SA as the 1st order kinetics, the plots of *ln C vs*. irradiation time for several catalytic samples were shown in Figure 4c. The overall decomposition trend in aqueous solution was quite similar as that of the reactions in gas phase. That is, the composite of 47/53 BiOCl/Bi_3O_4Cl showed the highest photocatalytic activity.

Both BiOCl and Bi_3O_4Cl showed very low photocatalytic activity under a visible light irradiation, but their heterojunctions demonstrated much higher activity than the end-members. The unusually high photocatalytic activity of BiOCl/Bi_3O_4Cl would be closely related to the unique relative band positions of these two semiconductors. The calculation of the energy band in our previous work revealed that the VB position of Bi_2O_3 was lower than that of BiOCl by 0.7 eV.[15] This seems to be a reasonable result, since VB of Bi_2O_3 originates from O 2p, whereas that of BiOCl mainly comes from Cl 3p.[22,23] It is also deduced that the increase of Cl component in the bismuth oxychloride family raises the VB position. The exact energy band position of Bi_3O_4Cl, utilized as a sensitizer in this work, has not been reported thus far, but its VB position can be estimated from the data for Bi_2O_3 and BiOCl. That is, the VB level of Bi_3O_4Cl will be located in the middle of that of Bi_2O_3 and BiOCl, suggesting that the VB level of Bi_3O_4Cl is located lower than that of BiOCl. Hence, the BiOCl/Bi_3O_4Cl system could be a Type-B heterojunction photocatalyst.[15,24-26] With irradiation of visible light, the electrons in VB of Bi_3O_4Cl are excited to its CB. Thereby VB of Bi_3O_4Cl is rendered partially vacant, and the electrons in VB of BiOCl can be transferred to that of Bi_3O_4Cl. As a result, holes are generated in VB of BiOCl, and these can initiate photocatalytic oxidation reactions. Therefore, with the irradiation of visible light, the BiOCl/Bi_3O_4Cl system can induce complete mineralization of organics.

Conclusions

A new visible light photocatalyst was formed by the heterojunction between BiOCl and Bi_3O_4Cl. The BiOCl/Bi_3O_4Cl composites showed a considerable photocatalytic activity in decomposing gaseous IP and aqueous SA, and the highest efficiencies were observed for 47/53 BiOCl/Bi_3O_4Cl. It is considered that the enhanced photocatalytic efficiency originates from the relative energy band positions of these two semiconductors, and the considerable absorbance of visible light by Bi_3O_4Cl. Relatively lower VB level of Bi_3O_4Cl than that of BiOCl enables the hole transfer from VB of Bi_3O_4Cl to that of BiOCl. As a result, the holes are generated in VB of BiOCl, which leads to the complete mineralization of organic compounds.

Acknowledgments. The authors gratefully acknowledge the financial support of the Ministry of Environment, Republic of Korea (Project No. 2009-02002-0051-0), and National Research Foundation of Korea (Project No. 2009-0076463).

References

1. Zou, Z.; Ye, J.; Sayama, K.; Arakawa, H. *Nature* **2001**, *414*, 625.
2. Xu, T. G.; Zhang, C.; Shao, X.; Wu, K.; Zhu, Y. F. *Adv. Funct. Mater.* **2006**, *16*, 1599.
3. Ipe, B. I.; Niemeyer, G. M. *Angew. Chem. Int. Ed.* **2006**, *45*, 504.
4. Hoffmann, M. R.; Martin, S. T.; Choi, W.; Bahnemann, D. W. *Chem. Rev.* **1995**, *95*, 69.
5. Tachikawa, T.; Tojo, S.; Fujitsuka, M.; Majima, T. *Chem. Eur. J.* **2006**, *12*, 3124.
6. Murase, T.; Irie, H.; Hashimoto, K. *J. Phys. Chem. B* **2005**, *109*, 13420.
7. Hou, Y.; Wang, X.; Wu, L.; Ding, Z.; Fu, X. *Environ. Sci. Technol.* **2006**, *40*, 5799.
8. Alvaro, M.; Aprile, C.; Benitez, M.; Carbonell, E.; García, H. *J. Phys. Chem. B* **2006**, *110*, 6661.
9. Zhang, Y.; Li, J.; Wang, J. *Chem. Mater.* **2006**, *18*, 2917.
10. Han, S.; Choi, S.-H.; Kim, S.-S.; Cho, M.; Jang, B.; Kim, D.-Y.; Yoon, J.; Hyeon, T. *Small* **2005**, *1*, 812.
11. Yao, W.; Wang, H.; Xu, X.; Shang, S.; Hou, Y.; Zhang, Y.; Wang, M. *Mater. Lett.* **2003**, *57*, 1899.
12. Wang, W.; Huang, F.; Lin, X. *Scripta Mater.* **2007**, *56*, 669.
13. Lin, X. P.; Huang, T.; Huang, F. Q.; Wang, W. D.; Shi, J. L. *J. Phys. Chem. B* **2006**, *110*, 24629.
14. Zhang, K. L.; Liu, C. M.; Huang, F. Q.; Zheng, C.; Wang, W. D. *Appl. Catal. B: Environ.* **2006**, *68*, 125.
15. Chai, S. Y.; Kim, Y. J.; Jung, M. H.; Chakraborty, A. K.; Jung, D.; Lee, W. I. *J. Catal.* **2009**, *262*, 144.
16. Kwon, Y. T.; Song, K. Y.; Lee, W. I.; Choi, G. J.; Do, Y. R. *J. Catal.* **2000**, *191*, 192.
17. Zhang, H.; Banfield, J. F. *J. Phys. Chem. B* **2000**, *104*, 3481.
18. Zhang, L.; Wang, W.; Yang, J.; Chen, Z.; Zhang, W.; Zhou, L.; Liu, S. *Appl. Catal. A: Gen.* **2006**, *308*, 105.
19. Ginley, D. S.; Butler, M. A. *J. Appl. Phys.* **1977**, *48*, 2019.
20. Ezema, F. I. *Pac. J. Sci. Tech.* **2005**, *6*, 6.
21. Kudo, A.;Omori, K.; Kato, H. *J. Am. Chem. Soc.* **1999**, *121*, 11459.
22. Fu, W. T. *Physica C* **1995**, *250*, 67.
23. Oshikiri, M.; Boero, M.; Ye, J.; Zou, Z.; Kido, G. *J. Chem. Phys.* **2002**, *117*, 7313.
24. Gao, B.; Kim, Y. J.; Chakraborty, A. K.; Lee, W. I. *Appl. Catal. B: Environ.* **2008**, *83*, 202.
25. Kim, Y. J.; Gao, B.; Han, S. Y.; Jung, M. H.; Chakraborty, A. K.; Ko, T.; Lee, C.; Lee, W. I. *J. Phys. Chem. C* **2009**, *113*, 19179.
26. Rawal, S. B.; Chakraborty, A. K.; Lee, W. I. *Bull. Korean Chem. Soc.* **2009**, *30*, 2613.